

# SFitter: Reconstructing the MSSM Lagrangian from LHC data

M. Rauch<sup>1</sup>, R. Lafaye<sup>2</sup>, T. Plehn<sup>1</sup>, and D. Zerwas<sup>3</sup>

<sup>1</sup> SUPA, School of Physics, University of Edinburgh, Scotland

<sup>2</sup> LAPP, Université Savoie, IN2P3/CNRS, Annecy, France

<sup>3</sup> LAL, Université Paris-Sud, IN2P3/CNRS, Orsay, France

**Abstract.** Once supersymmetry is found at the LHC, the question arises what are the fundamental parameters of the Lagrangian. The answer to this question should thereby not be biased by assumptions on high-scale models. SFitter is a tool designed for this task. Taking LHC (and possibly ILC) data as input it scans the TeV-scale MSSM parameter space using its new weighted Markov chain technique. Using this scan it determines a list of best-fitting parameter points. Additionally a log-likelihood map is calculated, which can be reduced to lower-dimensional Frequentist's profile likelihoods or Bayesian probability maps.

**PACS.** 02.50.Fz Stochastic analysis – 12.60.Jv Supersymmetric models

## 1 Introduction

The search for a Higgs boson, or to find an alternative to such a fundamental scalar, are the main goals of the LHC, which will start operation next year. However, the Higgs-boson mass is quadratically divergent with the cutoff scale of the theory, and the question about possible ultraviolet completions of the Standard Model arises. Such a completion should also provide an answer for the second unsolved question in high-energy physics, the existence of cold dark matter.

One possible, and particularly attractive, extension of the Standard Model is supersymmetry. Its parameter space has been constrained by various sources over the last years. Collider data from LEP and Tevatron have put stringent bounds on the masses of the superparticles both via direct and indirect searches, like the mass of the lightest Higgs boson, and indirect measurements like the anomalous magnetic moment of the muon have put further restrictions on the parameter space. Also there is no one-to-one correspondence of observables and parameters. This is especially true once we take loop-corrections into account. At the same time as few assumptions as possible should be imposed. They should instead be inferred from the available data.

The program SFitter [1] is designed to solve the task of mapping up to 20-dimensional highly complex parameter spaces onto a large set of observables of different quality, which can be highly correlated. In this proceedings we discuss the techniques and options of SFitter. The experimentally well-studied MSUGRA parameter point SPS1a [2] is thereby used as an example to illustrate the features and physical results of this parameter point.

## 2 Tools and Techniques

SFitter can use data input from both high-energy colliders and low-energy constraints. Possible choices include kinematic endpoints and thresholds which appear in invariant-mass distributions, mass differences and masses themselves. Furthermore, it is possible to use branching ratios and cross sections. The latter ones are normally associated with large errors, so one would rely on them only when there are no other types of measurements available. But from a technical point of view large error bars pose no problem to SFitter. It is even possible to consider data from e.g. ATLAS and CMS measurements separately.

This data is then compared to the theoretical predictions. Starting from a parameter point the physical spectrum is calculated by a choice of three spectrum generators, SoftSUSY [3], SuSPECT [5] or ISASUSY [4]. Next-to-leading-order cross sections for LHC or a future ILC are calculated by the program Prospino2 [6] and branching ratios can be included via links to Msmlib [7] and SUSY-HIT [8]. Also the dark matter content of the relic density is readily available by an interface to micrOMEGAs [9]. The communication of parameters and results between the different programs is performed by the SUSY-Les-Houches-Accord [10] data format using the implementation of SLHAio [11].

Comparing the experimental data  $d_i$  and the theoretical prediction  $\bar{d}_i$ , where the index  $i$  runs over the different data, a likelihood value is assigned to every point in parameter space. Hereby we follow the RFit scheme of CKMFitter as described in Ref. [12] and assume the theoretical errors  $\sigma_i^{\text{theo}}$  as box-shaped. This scheme interprets theoretical errors as a lack of knowledge on a parameter. As long as the deviation between

theory and experiment is within the theoretical error, this must not have any influence on the total likelihood. In combination with the experimental error  $\sigma_i^{\text{exp}}$  the total log-likelihood  $\log \mathcal{L} = -\frac{\chi^2}{2}$  is given by

$$\chi^2 = \begin{cases} 0 & \text{for } |d_i - \bar{d}_i| < \sigma_i^{\text{theo}} \\ \left( \frac{|d_i - \bar{d}_i| - \sigma_i^{\text{theo}}}{\sigma_i^{\text{exp}}} \right)^2 & \text{for } |d_i - \bar{d}_i| \geq \sigma_i^{\text{theo}} \end{cases} \quad (1)$$

The experimental error itself is a combination of three different sources. All three are considered to be gaussian and therefore are summed quadratically. The statistical error is assumed to be uncorrelated between different measurements. The first systematic error originates from the lepton energy scale. It is taken to be 99% correlated between different observables. The second one has its source in the jet energy scale and is taken with a 99% correlation as well.

To reconstruct Lagrangian parameters a scan of the parameter space is performed. This is not only important to obtain the correct solution, or possibly a set of solutions. It is also necessary to extract error estimates on the parameters from the data. To accomplish this goal a choice of three different methods is available, which can be freely combined. The first one is using a fixed grid. Secondly, Minuit [13] is included as a minimum finder, which employs a steepest-descent hill-climbing algorithm. The third option uses the technique of Weighted Markov Chains, which are described in more detail in the remainder of this section.

Markov chains are defined as a sequence of points which are the result of a stochastic process. The special, Markov, property which characterises them is that the conditional probability of each point only depends on its direct predecessor, but not on any other previous, or future, points in the chain. In SFitter the Metropolis-Hastings [14] algorithm is used for choosing the next point, which works in the following way. In the first part of the algorithm a new point is suggested based on the current one using a probability distribution function (PDF). The PDF can be freely chosen as long as it satisfies the property that the probability from being at point  $x$  and proposing  $x'$  is the same as being at  $x'$  and proposing  $x$ . It can for example be chosen flat, then the Markov-Chain algorithm has no dependence between points at all and reduces to a simple Monte-Carlo fitting. A good performance was found using a Breit-Wigner-, or Cauchy-, shaped function. This type of function has more pronounced tails than a gaussian distribution and provides a better balance to avoid random-walk behaviour. The second part of Metropolis-Hastings consists of the acceptance stage. It is decided whether the suggested point is accepted or rejected based on a potential, which in our case is  $\frac{1}{\chi^2}$ . So if the log-likelihood of the suggested point is larger than that of the old one, it is always accepted, else, it is accepted if the ratio of the two log-likelihoods is larger than a random number  $r$  chosen uniformly between 0 and 1. In all other cases the old

point is added to the Markov chain another time:

$$x_{\text{new}} = \begin{cases} x_{\text{sugg}} & \text{if } \log \mathcal{L}(x_{\text{sugg}}) > \log \mathcal{L}(x_{\text{old}}) \\ & \text{or } \log \mathcal{L}(x_{\text{sugg}}) / \log \mathcal{L}(x_{\text{old}}) > r, \\ x_{\text{old}} & \text{else.} \end{cases} \quad (2)$$

As a rule of thumb, an acceptance rate of 25% is generally considered optimal. The resulting Markov chain has the property that the density of points is proportional to the potential, i.e. to  $\frac{1}{\chi^2}$  which can then be used to obtain likelihood maps by binning the points. To do this binning we have developed a new algorithm [15] based on previous work by Ferrenberg and Swendsen [16]. This one does not just take every point with a weight of one, which corresponds to the classic way. As the function we want to plot is the same which has been used in the acceptance decision, this information can be reused. We therefore weight the points with the potential function taking care that no double-counting is done and points where the likelihood vanishes are properly taken into account.

It was shown [17] that Markov-chain techniques can scan high-dimensional parameter spaces very efficiently. They have been extensively applied to constrain the MSUGRA parameter space from current experimental precision data [18, 19].

### 3 Reconstructing SPS1a

With these possibilities SFitter provides the relevant frequentist or Bayesian results in three steps: First, a fully exclusive log-likelihood map of the complete parameter space is calculated. In a second step the best local likelihood maxima are obtained from the map and ranked according to their likelihood. Last, the map is projected onto lower-dimensional spaces down to one-dimensional distributions. This can be done in both a Frequentist way, which yields a profile likelihood, and in a Bayesian way. Here the unwanted dimensions are marginalised away and a prior needs to be specified for this.

In general, no specific model for supersymmetry breaking should be assumed a priori. Instead this should be inferred from the data. However, to demonstrate the features of SFitter we consider here the MSUGRA scenario using the parameter point SPS1a. Besides the MSUGRA parameters  $m_0$ ,  $m_{1/2}$ ,  $\tan \beta$ ,  $A_0$  and  $\text{sgn} \mu$  also the top-quark mass  $m_t$  is taken as a free parameter because of the large uncertainty on its value. A smeared dataset is generated from the measurements which can be performed in this parameter point. Using 30 individual chains with 20000 points each a Weighted Markov run is used to produce the likelihood map. For the best points an additional Minuit fit is performed to find the exact position of the minimum. With this procedure we find four distinct minima as shown in Table 1. The best point corresponds indeed to the true solution where the deviations turn out to be compatible with the error bars. The second solution is given by very similar values for the continuous parameters

| $\chi^2$ | $m_0$ | $m_{1/2}$ | $\tan\beta$ | $A_0$  | $\mu$ | $m_t$ |
|----------|-------|-----------|-------------|--------|-------|-------|
| 0.09     | 102.0 | 254.0     | 11.5        | -95.2  | +     | 172.4 |
| 1.50     | 104.8 | 242.1     | 12.9        | -174.4 | -     | 172.3 |
| 73.2     | 108.1 | 266.4     | 14.6        | 742.4  | +     | 173.7 |
| 139.5    | 112.1 | 261.0     | 18.0        | 632.6  | -     | 173.0 |
| ...      |       |           |             |        |       |       |
| errors   | 2.17  | 2.64      | 2.45        | 49.6   |       | 0.97  |

**Table 1.** SFitter output for the SPS1a point in MSUGRA. List of the best-fitting parameter points with associated log-likelihood. The last line denotes the corresponding errors for the best-fitting point. All masses are in units of GeV.

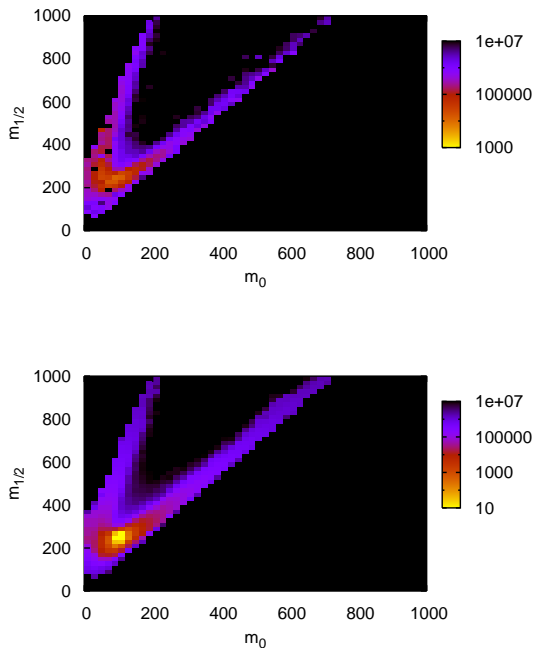


**Fig. 1.** SFitter output for the SPS1a point in MSUGRA. Two-dimensional likelihood maps of the  $m_0$ - $m_{1/2}$  plane. Upper: Bayesian marginalised plots. Lower: Profile likelihoods. All masses are given in GeV.

and a flipped sign of  $\mu$ . Solution three shows a distinct maximum, and the last one again differs from the previous one only by  $\text{sgn}\mu$ . For these last two solutions the trilinear parameter takes a large positive value together with a slight shift in the top-quark mass. If the latter was kept fixed this distinct maximum would be much less pronounced. In the last line of Table 1 the corresponding errors on the parameters are printed.

Fig. 1 shows the corresponding plots of the likelihood map projected onto the  $m_0$ - $m_{1/2}$  plane. The peak is clearly at the right position in both the marginalised plot and the profile likelihood. The resolution of the plots is too coarse so the different maxima are merged in a single bin and cannot be resolved here. From there it extends in two branches, which reflect the fact that extracting masses from kinematic endpoints involves quadratic equations.

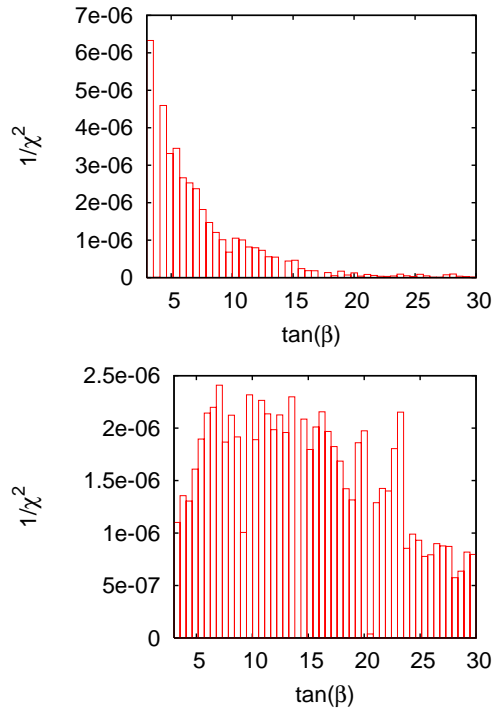


**Fig. 2.** SFitter output for the SPS1a point in MSUGRA. One-dimensional Bayesian marginalised plots for  $\tan\beta$ . Upper: High-scale prior flat in  $B$ . Lower: Prior flat in  $\tan\beta$ .

Strictly speaking, the usual set of MSUGRA parameter is not purely high-scale, as it contains the weak-scale quantity  $\tan\beta$  which explicitly assumes radiative electroweak symmetry breaking. This can be replaced by the mass parameters  $B$  and  $\mu$  [18] which appear as  $B\mu$  in front of mixed terms of the type  $H_1^0 H_2^0$ .  $\mu$  can then be eliminated by the requirement that the correct low-energy  $Z$ -boson mass is reproduced. This distinction is important for the marginalised plots, where a prior as a measure in the parameter space must be specified. Fig. 2 shows the different results of the two choices. In the upper plot a purely high-scale model is chosen as has been done in the previous plots. The prior is taken to be flat in  $B$ . This corresponds to a prior in  $\tan\beta$ , which falls off as  $1/\tan\beta^2$  in leading order. This behaviour is clearly visible in the plot. It is dominated by noise and the prior and as small values of  $\tan\beta$  as possible are preferred. In the lower plot a prior which is flat in  $\tan\beta$  has been chosen. Here the plot still shows a significant noise, but the maximum is in the correct place. For profile-likelihood plots this choice does not make a difference in the resulting likelihood. It does however have an indirect influence via the Markov chain scanning. For the PDF a measure in the parameter space must be defined which influences the probability for suggesting a point. A bad choice of the PDF can then lead to a bad coverage of the parameter space.

## 4 Dark Matter

A very important clue for Physics beyond the Standard Model is the existence of cold dark matter, which in the SM cannot be created in the right quantity. Supersymmetry provides an ideal candidate to solve this problem. The lightest neutralino as the lightest supersymmetric particle is stable, massive and only weakly interacting. That it is indeed responsible for the dark matter content of the universe is a hypothesis which should not just be simply assumed and used in the fits. Using future collider data it is possible to test it. After the Lagrangian parameters and their associated errors have been extracted, the relic density can then be computed and compared to the experimental data. In this short analysis we ignore the fact that SPS1a produces a too large density which is excluded and would overclose the universe, since we are not interested in the central values but in the principal dependence of the parameters and the propagation of the errors.

Using the information on the parameters obtained in the previous section we use micrOMEGAs to calculate an estimate of the relic density  $\Omega_{\text{CDM, SPS1a}} h^2 = 0.1906 \pm 0.0033$ . The amount decreases with smaller  $m_0$  and larger  $\tan\beta$ , while the dependence on  $m_{1/2}$  and  $A_0$  is rather weak. This can then be compared to the experimental value, which is derived from the measurement of the fluctuations of the cosmic microwave background by WMAP [20]. The current best value is  $\Omega_{\text{CDM, exp}} h^2 = 0.1277 \pm 0.008$ . Adding possible future ILC measurements would mean an additional error reduction in the extracted value by a factor of 10. So the accuracy which can be derived from collider data alone is well compatible with the experimental precision and testing the hypothesis that the lightest neutralino is responsible for the dark matter content of the universe viable.

## 5 Conclusions

If new physics is discovered at the LHC, the crucial task will be to map the possibly strongly correlated observables onto a high-dimensional weak-scale Lagrangian. SFitter with its new weighted Markov chain technique has been designed to accomplish such a task. It produces both a list of best points and a fully-dimensional exclusive likelihood map as output. The dimensionality of this map can then be reduced using either Frequentist or Bayesian techniques, which yield a profile likelihood or marginalised plots, respectively. The latter depend on the choice of priors, which can have a significant effect when the data cannot constrain parameters sufficiently and demonstrate Bayesian volume effects. After the reconstruction the parameter set can be used for a prediction of the relic density, which can then be compared to the experimental value. We find that for SPS1a both values have comparable errors. SFitter is despite its name not limited to supersymmetry. It can and will be used to study further problems involving high-dimensional parameter spaces.

## References

1. R. Lafaye, T. Plehn, M. Rauch and D. Zerwas, arXiv:0709.3985 [hep-ph].
2. B. C. Allanach *et al.*, in *Proc. of the APS/DPF/DPB Summer Study on the Future of Particle Physics (Snowmass 2001)* ed. N. Graf, Eur. Phys. J. C **25**, 113 (2002).
3. B. C. Allanach, Comput. Phys. Commun. **143**, 305 (2002).
4. H. Baer, F. E. Paige, S. D. Protopopescu and X. Tata, arXiv:hep-ph/9305342.
5. A. Djouadi, J. L. Kneur and G. Moultaka, arXiv:hep-ph/0211331.
6. T. Plehn *et al.*, Prospino2, <http://www.ph.ed.ac.uk/~tplehn/prospino/>.
7. G. Ganis, msmlib, <http://home.cern.ch/ganis/MSMLIB/msmlib.html>.
8. M. Mühlleitner, A. Djouadi and Y. Mambrini, arXiv:hep-ph/0311167; A. Djouadi, M. M. Mühlleitner and M. Spira, Acta Phys. Polon. B **38**, 635 (2007) [arXiv:hep-ph/0609292].
9. G. Belanger, F. Boudjema, A. Pukhov and A. Semenov, Comput. Phys. Commun. **176**, 367 (2007) [arXiv:hep-ph/0607059]; G. Belanger, F. Boudjema, A. Pukhov and A. Semenov, Comput. Phys. Commun. **174**, 577 (2006) [arXiv:hep-ph/0405253]; G. Belanger, F. Boudjema, A. Pukhov and A. Semenov, Comput. Phys. Commun. **149**, 103 (2002) [arXiv:hep-ph/0112278].
10. P. Skands *et al.*, JHEP **0407**, 036 (2004) [arXiv:hep-ph/0311123].
11. S. Kreiss (in preparation), see <http://www.svenkreiss.com/SLHAio>.
12. A. Höcker, H. Lacker, S. Laplace and F. Le Diberder, Eur. Phys. J. C **21**, 225 (2001); J. Charles, A. Höcker, H. Lacker, F. R. Le Diberder and S. T'Jampens, arXiv:hep-ph/0607246.
13. F. James, M. Roos, Comp. Phys. Commun. **10**, 343 (1975).
14. N. Metropolis, A.W. Rosenbluth, M.N. Teller and E. Teller, Journal of Chemical Physics, **21**, 1087 (1953); W.K. Hastings, Biometrika **57**, 97 (1970).
15. R. Lafaye, T. Plehn, M. Rauch, and D. Zerwas (in preparation).
16. A. M. Ferrenberg, R. H. Swendsen, Phys. Rev. Lett. **61**, 2635 (1988).
17. E. A. Baltz and P. Gondolo, JHEP **0410**, 052 (2004) [arXiv:hep-ph/0407039].
18. B. C. Allanach and C. G. Lester, Phys. Rev. D **73**, 015013 (2006); B. C. Allanach, Phys. Lett. B **635**, 123 (2006); B. C. Allanach, C. G. Lester and A. M. Weber, JHEP **0612**, 065 (2006) [arXiv:hep-ph/0609295]; B. C. Allanach, K. Cranmer, C. G. Lester and A. M. Weber, arXiv:0705.0487 [hep-ph].
19. R. R. de Austri, R. Trotta and L. Roszkowski, JHEP **0605**, 002 (2006); R. Trotta, R. Ruiz de Austri and L. Roszkowski, J. Phys. Conf. Ser. **60**, 259 (2007); R. Trotta, R. R. de Austri and L. Roszkowski, New Astron. Rev. **51**, 316 (2007); L. Roszkowski, R. R. de Austri, J. Silk and R. Trotta, arXiv:0707.0622 [astro-ph].
20. D. N. Spergel *et al.* [WMAP Collaboration], Astrophys. J. Suppl. **170**, 377 (2007) [arXiv:astro-ph/0603449].